Supplementary Information

Table of Contents

1 Extended figures and tables 2

1.1 Overview of root zone storage estimate methods (complement to Sect. 1 Introduction) 2

1.2 Soil moisture retention curve (complement to Sect. 2 Methods) 3

1.3 Precipitation and evaporation by river basin (complement to Sect. 3 Data) 4

1.4 Land cover map (complement to Sect. 3 Data) 5

1.5 Effect of input data on S_R (complement to Sect. 4.1) 6

1.6 Comparison to other root zone storage capacity estimates (complement to Sect. 4.2) 8

1.7 Differences in evaporation simulation with $S_{R,CHIRPS\text{-}CSM}$ (complement to Sect. 4.3) 9

2 Change of soil moisture stress function in STEAM 10

2.1 Methods 10

2.2 Results and discussion 11

3 Increasing performance in STEAM by Gumbel normalised S_R 12

3.1 Methods 12

3.2 Results and discussion 12

References 16

1 Extended figures and tables

1.1 Overview of root zone storage estimate methods (complement to Sect. 1 Introduction)

Table S1. Overview of rooting depth or root zone storage capacity estimate methods. See also Sect. 1.1.

	Field observation based	**Look-up table**	**Optimisation approach**	**Inverse modelling**	**Calibration**	**Mass balance based**
Estimated variable	Actual root depths/profiles	Root zone storage capacity	(Hydrological) active root profiles	(Potential) hydrological active root depth	Hydrological root zone storage capacity	Hydrological root zone storage capacity
Spatial scale	Local, regional, global (scaled up from field observations)	Regional, global	Local (Potential for scaling up)	Global/regional	Catchment (transferable to global scale by regionalisation)	Catchment, regional, global
Type of model or algorithm	Mean biome, regression model	N/A	Analytical, stochastic, genetic algorithm	Vegetation model	Hydrological model	Mass curve technique or cumulative mass balance
Required input data	Regression model requires climate, soil, and vegetation information	Literature rooting depth, soil texture data	Climate, soil, and vegetation information	Climate, soil, and vegetation information	Climate and hydrological data	Runoff and/or evaporation demand, and precipitation
Main merits	- observation based	- grounded in literature - facilitates land cover change experiments	- improves understanding of root distribution development	- Earth observation based	- compensates for model uncertainties	- observation based - no need for soil and vegetation data - model independent
Main limitations	- Limited coverage of observations - possible need to convert to active root zone storage capacity	- assumes that a single rooting depth is valid across a land cover type	- model dependent - detailed input data required	- model and data dependent	- model and data dependent - parameter equifinality	- dependent on hydrological data
References (examples)	(Canadell et al., 1996; Jackson et al., 1996; Schenk and Jackson, 2009)	(Müller Schmied et al., 2014; Wang-Erlandsson et al., 2014)	(Collins and Bras, 2007; Laio et al., 2006; Schenk, 2008; van Wijk and Bouten, 2001)	(Ichii et al., 2007; Kleidon, 2004)	(Fenicia et al., 2009; Winsemius et al., 2009)	(de Boer-Euser et al., 2016; van Dijk et al., 2014; Gao et al., 2014), this study.

1.2 Soil moisture retention curve (complement to Sect. 2 Methods)

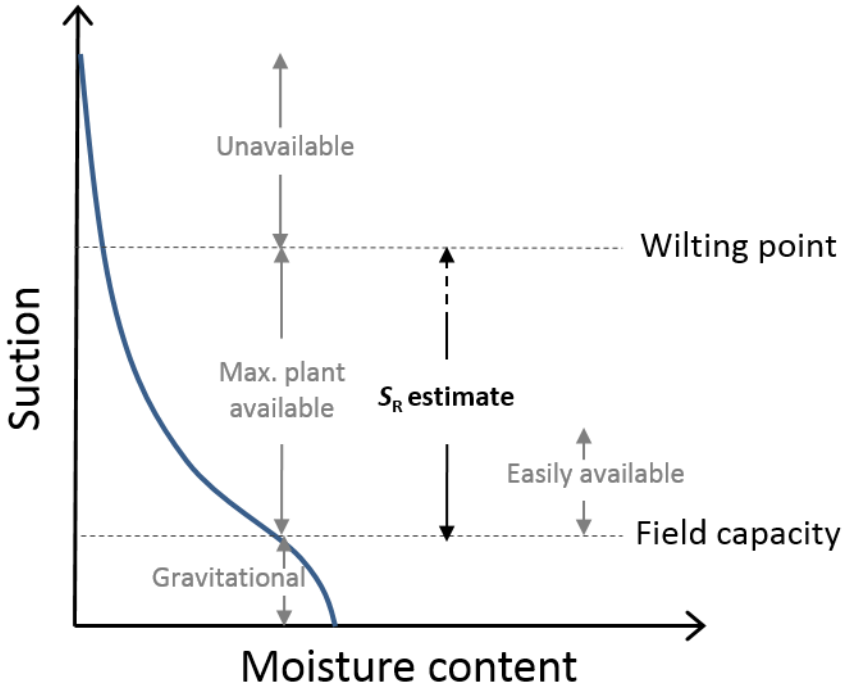

Figure S1. S_R estimate on the soil moisture retention curve. Ideally, the root zone storage capacity S_R correspond to the maximum plant available water. In case of a prolonged drought where all soil moisture is depleted. The estimated S_R is likely larger than the easily available moisture content and close to the maximum plant available moisture content. See also Sect. 2.1.

1.3 Precipitation and evaporation by river basin (complement to Sect. 3 Data)

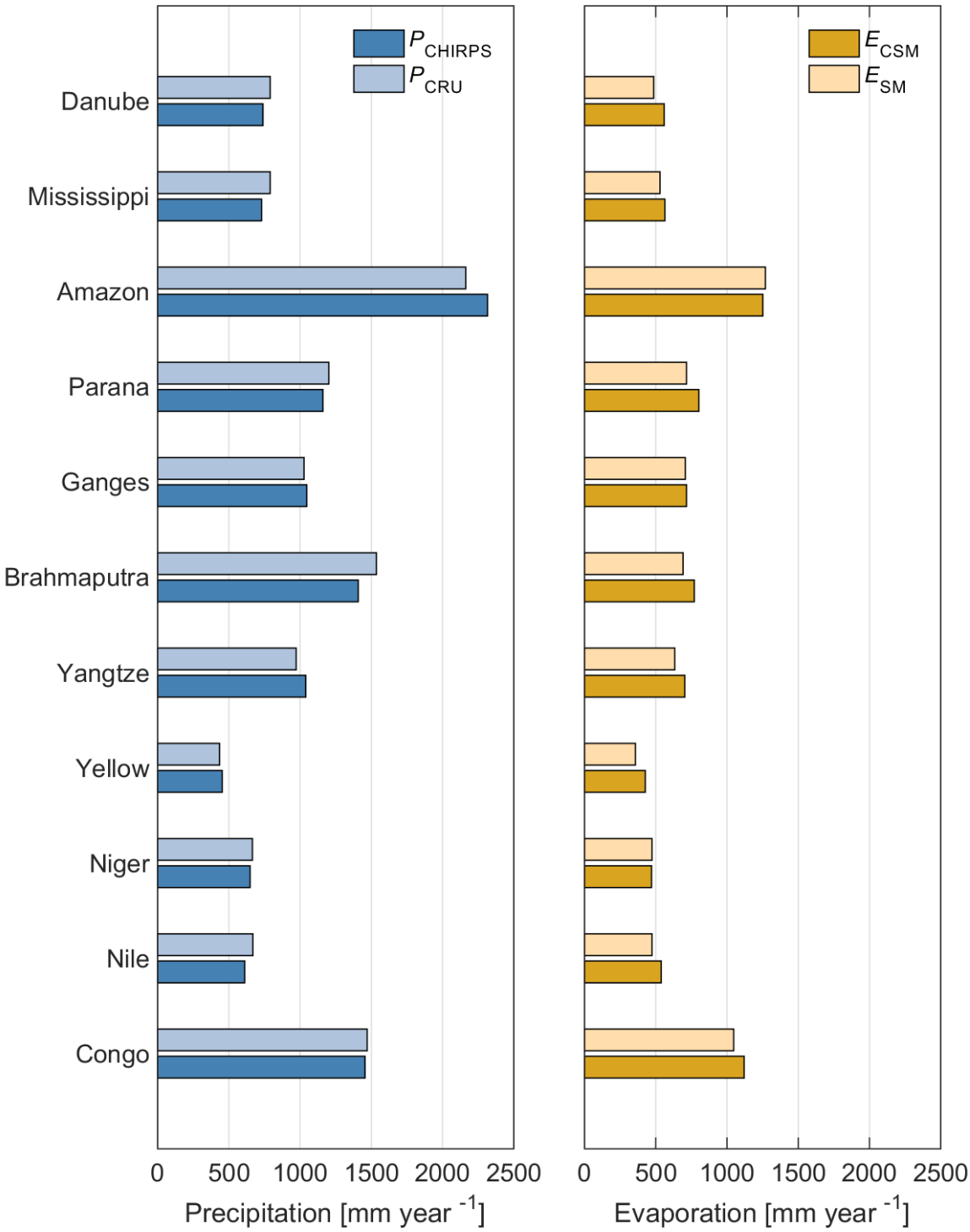

Figure S2. Mean annual precipitation and evaporation by river basins. See also Sect. 3.1.

1.4 Land cover map (complement to Sect. 3 Data)

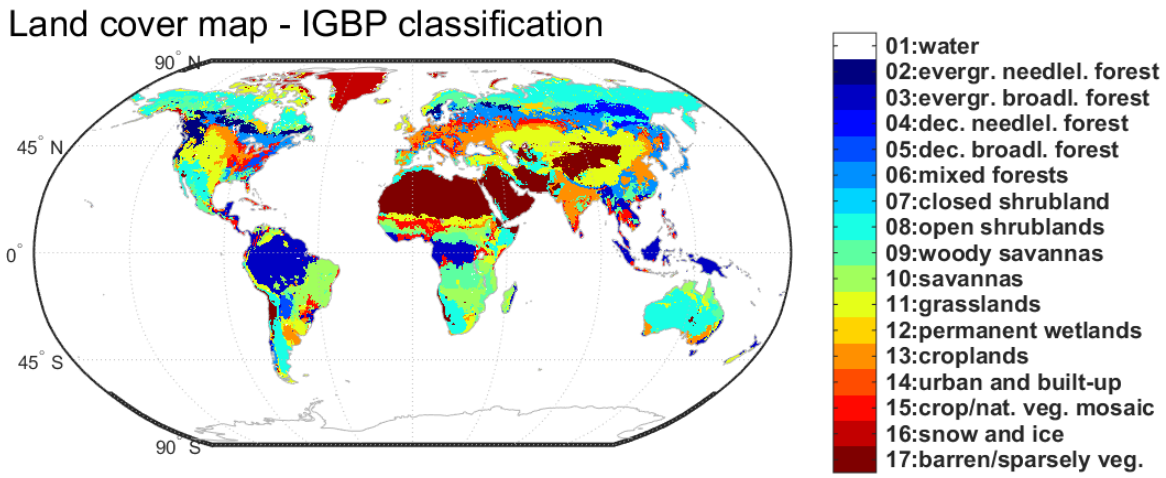

Figure S3. Land cover map (MCD12C1 from MODIS) used in this study showing the dominant land cover type in each grid cell.

1.5 Effect of input data on S_R (complement to Sect. 4.1)

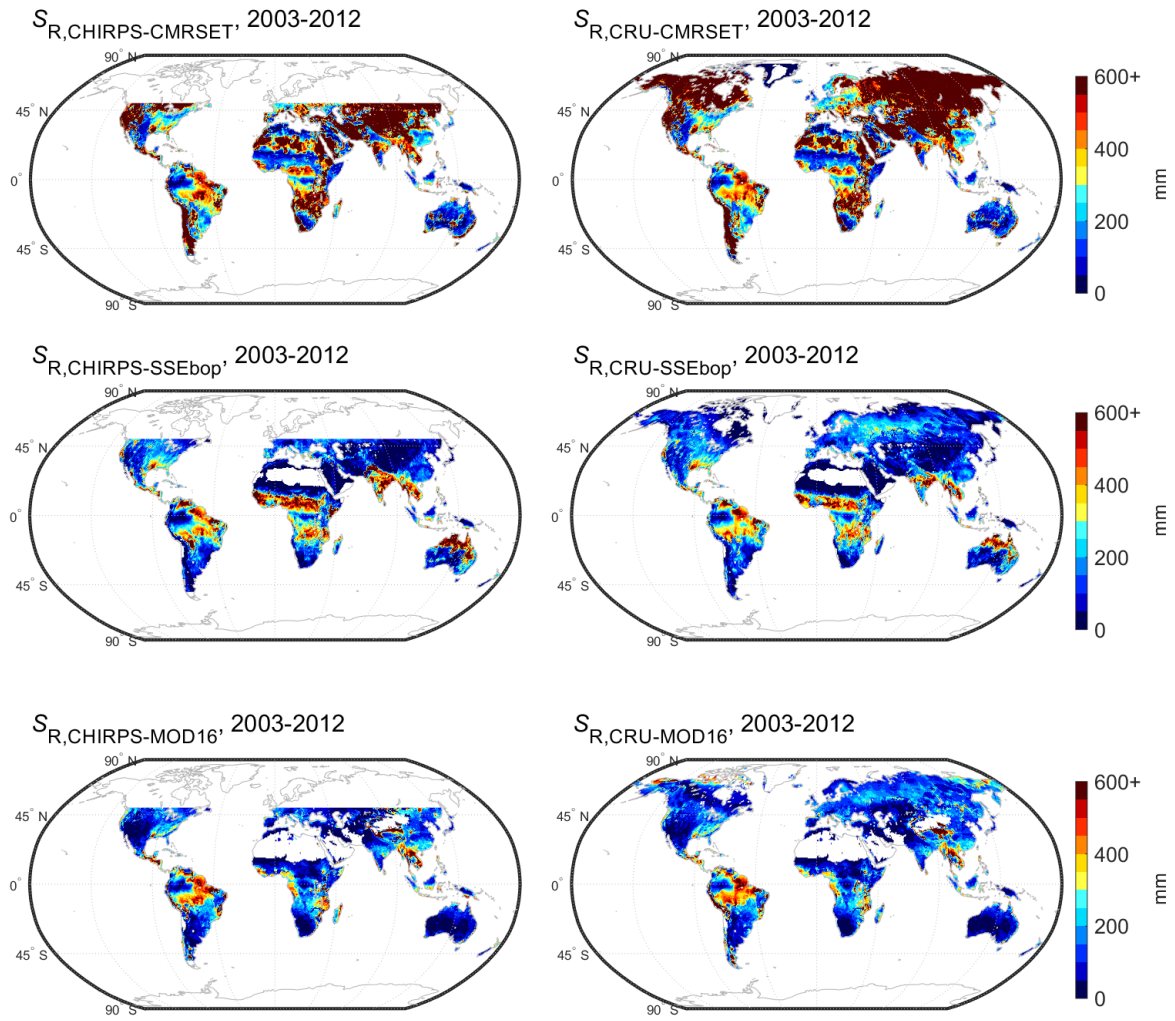

Figure S4. Root zone storage capacities derived using the different evaporation (CMSRET, SSEBop, MOD16) and precipitation (CHIRPS, CRU) datasets separately.

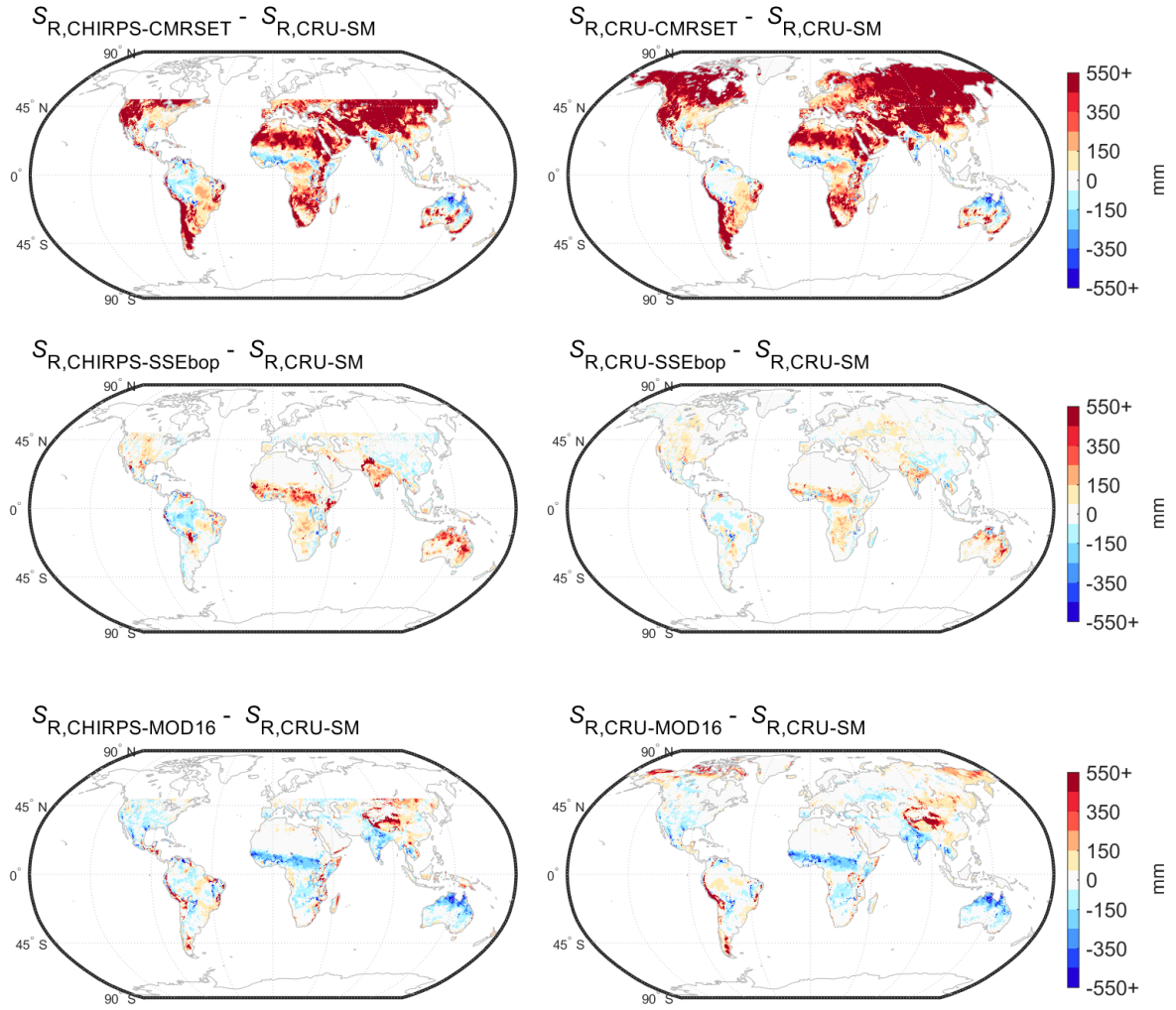

Figure S5. Differences between the root zone storage capacities derived using separate evaporation datasets and the ensemble evaporation derived global root zone storage capacity $S_{R,CRU\text{-}SM}$.

1.6 Comparison to other root zone storage capacity estimates (complement to Sect. 4.2)

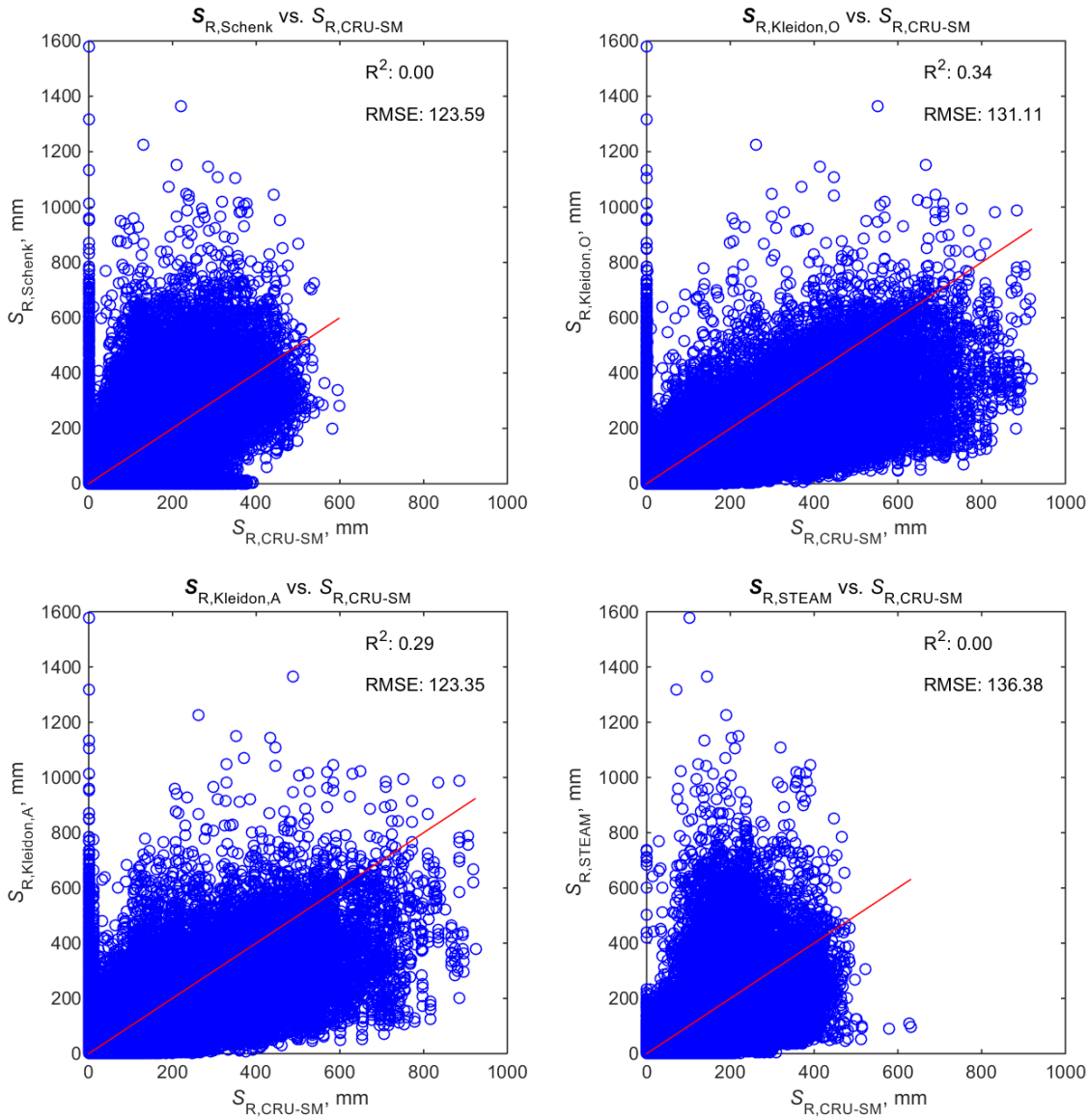

Figure S6. Comparison between root zone storage capacity estimates from other studies and this study ($S_{R,CRU-SM}$). The 1:1 line is in red.

Table S2. Root mean square errors (mm) between root zone storage capacity estimates from different studies.

	$S_{R,Schenk}$	$S_{R,Kleidon,O}$	$S_{R,Kleidon,A}$	$S_{R,STEAM}$	$S_{R,CRU-SM}$
$S_{R,Schenk}$					
$S_{R,Kleidon,O}$	147				
$S_{R,Kleidon,A}$	136	87			
$S_{R,STEAM}$	116	158	151		
$S_{R,CRU-SM}$	124	131	123	136	

1.7 Differences in evaporation simulation with $S_{R,CHIRPS\text{-}CSM}$ (complement to Sect. 4.3)

Root mean square error (ε_{RMS}) improvements in simulated mean annual evaporation (i.e., the increase in similarity between a benchmark evaporation products E_{CSM} or E_{SM} and the simulated E by using $S_{R,CRU\text{-}SM}$ or $S_{R,CHIRPS\text{-}CSM}$ instead of $S_{R,STEAM}$ as input to STEAM) are shown in Figure S7. The ε_{RMS} improvements in E simulation are very similar between the different setups, and mostly positive. The simulations are most similar to each other in the tropical belt, but diverges mildly in the multitudes, and shows a performance decrease towards the south when E_{CSM} is used as benchmark. The performance decreases in the far south may be related to the underperformance of CMRSET (i.e., a constituent evaporation product of E_{CSM}) in the high latitudes.

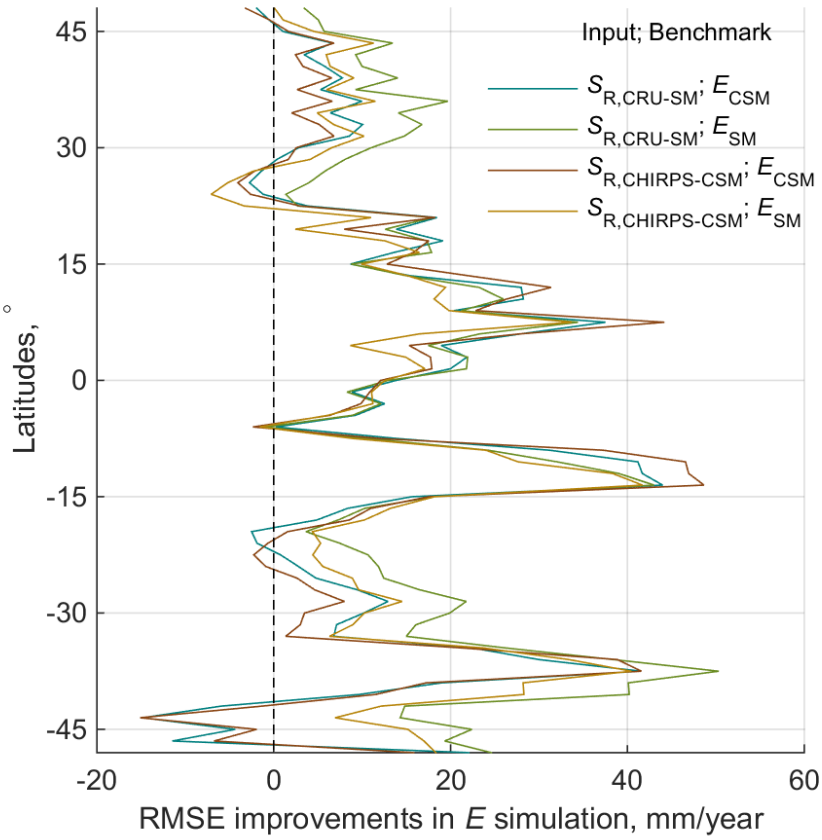

Figure S7. Root mean square error (ε_{RMS}) improvements of E simulation achieved by using $S_{R,CRU}$ and $S_{R,CHIRPS}$ as input to STEAM instead of $S_{R,STEAM}$. E_{CSM} and E_{SM} were used as benchmark for measuring improvements. See also Sect. 4.3.

2 Change of soil moisture stress function in STEAM

2.1 Methods

In the original version of STEAM (Wang-Erlandsson et al., 2014), the soil moisture stress function used was:

$$f(\theta) = \frac{(\theta - \theta_{\mathrm{wp}})(\theta_{fc} - \theta_{\mathrm{wp}} + c)}{(\theta_{fc} - \theta_{\mathrm{wp}})(\theta - \theta_{\mathrm{wp}} + c)} \ , \tag{S1}$$

where θ is the actual volumetric soil moisture content (dimensionless), θ_{wp} is the volumetric soil moisture content at wilting point, θ_{fc} at field capacity, and c is a soil moisture stress parameter assumed to be 0.07 (Matsumoto et al., 2008; Wang-Erlandsson et al., 2014).

We changed the soil moisture stress function in STEAM in order to remove the arbitrariness of choosing a soil moisture stress parameter. Instead, we use (van Genuchten, 1980)'s function for dimensionless water content:

$$f(\theta) = \frac{\theta - \theta_{wp}}{\theta_{fc} - \theta_{wp}} \ . \tag{S2}$$

To use the root zone storage capacity S_{R} instead of soil moisture content θ, we do not account for soil moisture below wilting point and assume $S_{\mathrm{R}} = h(\theta_{\mathrm{fc}} - \theta_{\mathrm{wp}})$, where h is the rooting depth (m). The reformulated stress function of soil moisture becomes:

$$f(\mathrm{S}) = \frac{S}{S_R} \ . \tag{S3}$$

In the original version of STEAM, the land cover specific rooting depth h_{lu} from a look-up table was used to simulate the land cover specific evaporation contribution, before the total evaporation was calculated based on the contributions from each land cover type. However, since S_{R} is location-bound and not land cover specific (i.e., soil moisture stress function in STEAM becomes based on location instead of land cover type), we defined a root zone storage $S_{\mathrm{R,steam}}$ (used in the main manuscript, see Sect 3.2) that is based on the look-up table based rooting depth:

$$S_{\mathrm{R,STEAM}} = h_{STEAM}(\theta_{\mathrm{fc}} - \theta_{\mathrm{wp}}) \ . \tag{S4}$$

The rooting depth map (h_{STEAM}) is derived by area-weighting the look-up table rooting depths with the land cover type fractional area coverage in each grid cell:

$$h_{\mathrm{STEAM}} = \sum_{lu=1}^{lu=17} h_{lu}\varphi_{lu} \ . \tag{S5}$$

where lu is land cover type, and ϕ_{lu} is the fractional grid cell coverage of land cover type lu. As evident from above equations, Eq. S2 and S3 are equivalent if h_{STEAM} is used in Eq. S2.

Thus, for the comparisons below, the rooting depth map h_{STEAM} is used as input to the Matsumoto formulation (Eq. S1), whereas $S_{\mathrm{R,steam}}$ is used as input to the van Genuchten root zone storage based formulation (Eq. S3). Therefore, the Matsumoto simulation here do not exactly correspond to the presented results in (Wang-Erlandsson et al., 2014). In the section below, we compare the evaporation simulation of STEAM depending on the soil moisture stress formulation used.

2.2 Results and discussion

Figure S8 and Table S3 compare the STEAM-simulated evaporation when using, on the one hand, the Matsumoto soil moisture stress function (Eq.S1), and, on the other, the van Genuchten equation (Eq. S3). The Matsumoto formulation leads to larger evaporation at places, particularly in the Sahel in January and in the eastern parts of the Amazon in July. This is logical, since van Genuchten assumes soil moisture stress to occur immediately when soil moisture content drops below field capacity, whereas the soil moisture stress curve dampens this effect in the Matsumoto formulation.

Table S3. Overview of STEAM-simulated mean annual evaporation and transpiration ratio (2003-2013) depending on the soil moisture stress function taken from Matsumoto et al., (2008) **or** van Genuchten, (1980)**.**

Soil moisture stress function	E (km^3/yr)	Transpiration ratio (%)
Matsumoto - h_{STEAM} (Eq. S1)	73,418	57.4
Van Genuchten - $S_{R,STEAM}$ (Eq. S3)	71,454	56.5

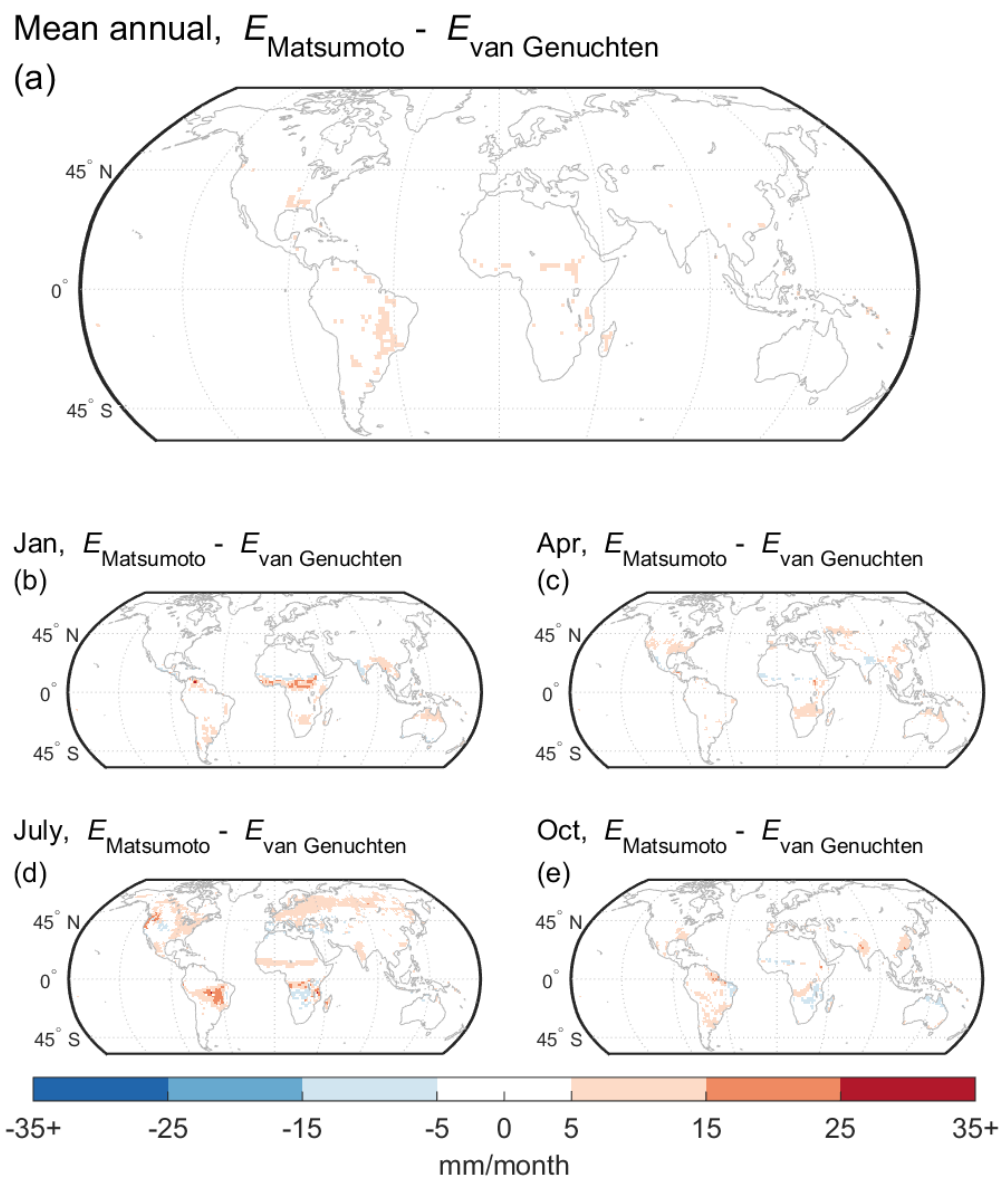

Figure S8. Difference in STEAM-simulated evaporation between using Matsumoto and Van Genuchten soil moisture stress formulation in STEAM (a) mean annual scale and averages for the months of (b) January, (c) April, (d) July, and (e) October over the time period 2003-2013.

3 Increasing performance in STEAM by Gumbel normalised S_R

3.1 Methods

As shown in Sect. 4.4, different land cover types seemed to increase E simulation in STEAM by Gumbel normalisation with different drought return years. A drought return period of 2 years ($S_{R,CRU-SM,2yrs}$) offers the best evaporation simulation performance in croplands, grasslands, open shrublands, barren land, and deciduous broadleaf forest, whereas it tends to decrease the model performance in other forest types. Instead, $S_{R,CRU-SM,10yrs}$ offers the highest performance in woody savannahs and savannahs, $S_{R,CRU-SM,20yrs}$ are by margin the best for evergreen needleleaf forest, and $S_{R,CRU-SM,60yrs}$ are best in evergreen broadleaf forests, deciduous needleleaf forest, and mixed forest.

Thus, we create a root zone storage capacity map $S_{R,CRU-SM,merged}$ that uses different drought return periods for different land cover types to increase performance in STEAM in principal based on Fig. 8. in Sect. 4.4. For water, urban land, and snow, where root zone storage capacity is not important, no Gumbel normalisation was applied. Table S4 shows the drought return periods matched to the different land cover types.

Table S4. The drought return period applied to the different land cover types.

S_R	Land cover type
$S_{R,CRU-SM,2yrs}$	05:deciduous broadleaf forest, 07:closed shrubland, 08:open shrublands, 11:grasslands,12:permanent wetlands,13:croplands, 15:cropland/natural veg. mosaic,17:barren or sparsely vegetated
$S_{R,CRU-SM,10yrs}$	09:woody savannas, 10:savannas
$S_{R,CRU-SM,20yrs}$	02:evergreen needleleaf forest
$S_{R,CRU-SM,60yrs}$	03:evergreen broadleaf forest, 04:deciduous needleleaf forest, 06:mixed forests
$S_{R,CRU-SM}$	01:water, 14:urban and built-up, 16:snow and ice

3.2 Results and discussion

Overall, the total mean annual evaporation are not changed significantly by the use of the different root zone storage capacities $S_{R,STEAM}$, and $S_{R,CRU-SM}$, but decreases by about 950-1040 km^3/year with $S_{R,CRU-SM,merged}$. Transpiration ratio decreases more than total evaporation, i.e., by about 1-2 percentage points (or 1450-1850 km^3/year), see Table S5.

Table S5. Overview of STEAM-simulated mean annual evaporation and transpiration ratio (2003-2013) depending on the input root zone storage capacity $S_{R,STEAM}$, $S_{R,CRU-SM}$, or $S_{R,CRU-SM,merged}$.

S_R input to STEAM	E (km^3/yr)	Transpiration ratio (%, km^3/yr)
$S_{R,STEAM}$	71,450	56.5 (40,370)
$S_{R,CRU-SM}$	71,370	56.0 (39,960)
$S_{R,CRU-SM,merged}$	70,420	54.7 (38,520)

Figure S9 shows a comparison between $S_{R,CRU-SM}$ (the maximum value of the time series 2003-2013) and $S_{R,CRU-SM,merged}$ (Gumbel normalisation with different drought return periods for different land cover types). The Gumbel normalisation reduces root zone storage capacity particularly in northern Australia, northern India, Bolivia, Argentina, south-eastern U.S., and Somalia. Increases are prominent in particularly in the Amazon, but also in Congo, tropical Southeast Asia, and Russia.

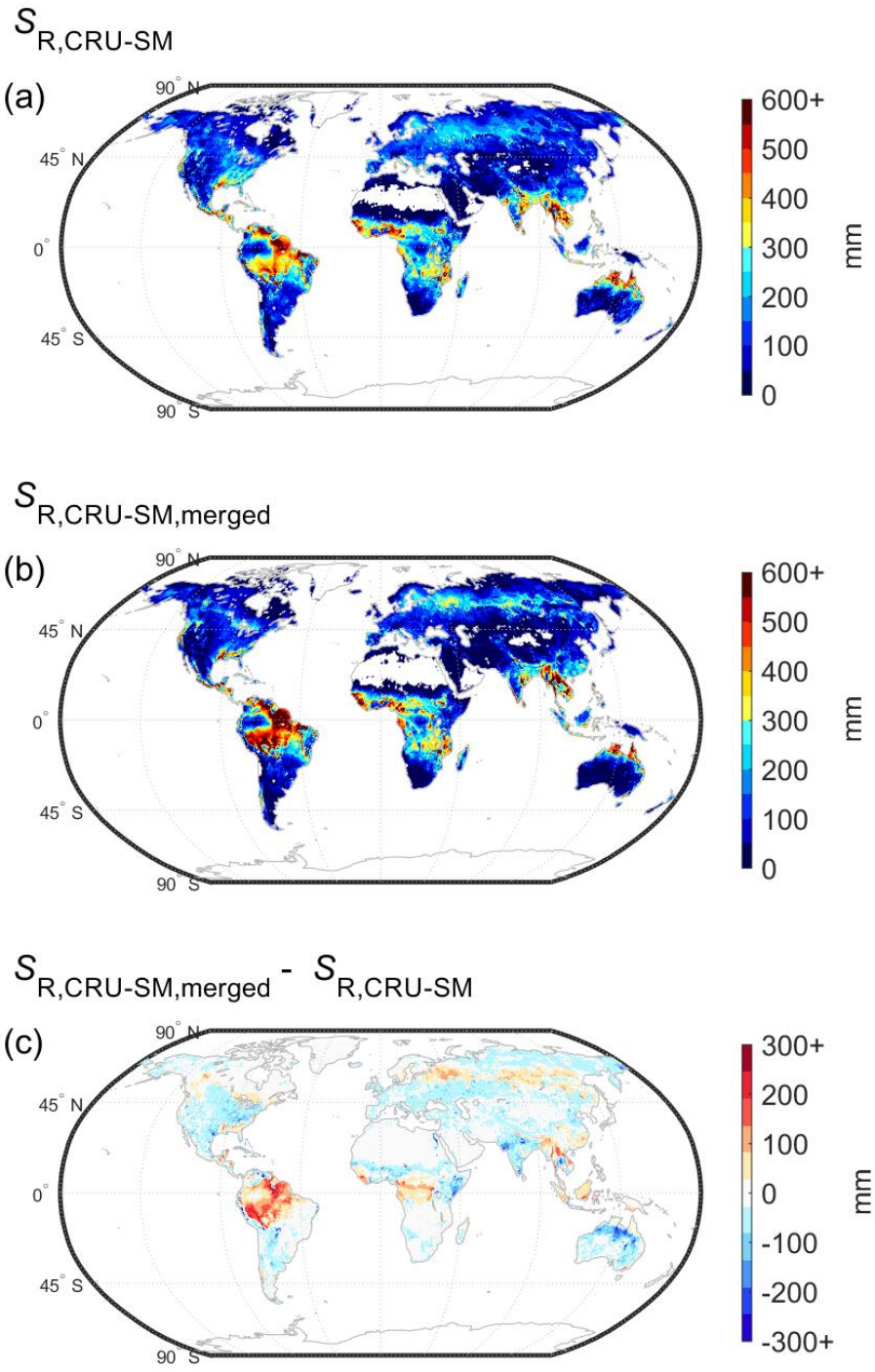

Figure S9. The (a) $S_{R,CRU-SM}$ (maximum storage deficit over the years 2003-2013), (b) $S_{R,CRU-SM,merged}$ (merged using the best performing Gumbel normalised S_R for each land cover type), and (c) the difference $S_{R,CRU-SM}$ and $S_{R,CRU-SM,merged}$.

Figure S10 compares the STEAM-simulated evaporation when using, on the one hand, $S_{R,CRU-SM,merged}$ and, on the other, the look-up table based $S_{R,STEAM}$. Similar to $S_{R,CRU-SM}$ (Fig. S11), $S_{R,CRU-SM,merged}$ has the greatest potential to influence model simulations for the hot and dry seasons, and for the seasonal tropical forests where the root zone storage capacity varies strongly. Compared to $S_{R,CRU-SM}$ (Fig. S11), $S_{R,CRU-SM,merged}$ causes at places greater reductions in seasonal evaporation (e.g., South America in January, and North America in July).

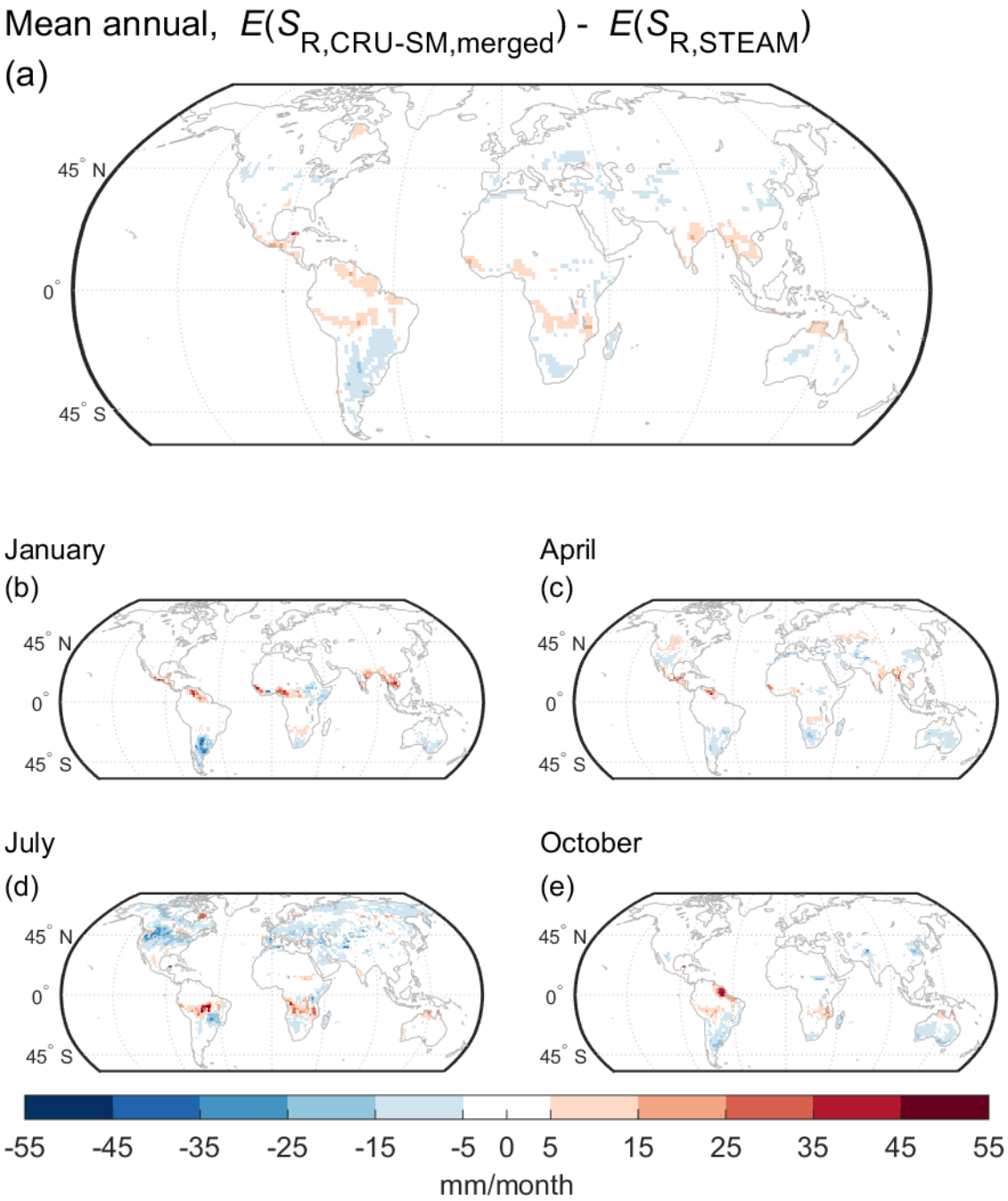

Figure S10. Difference in STEAM-simulated evaporation between using $S_{R,CRU\text{-}SM,merged}$ and $S_{R,STEAM}$ as root zone storage capacity parametrisation at (a) mean annual scale and averages for the months of (b) January, (c) April, (d) July, and (e) October over the time period 2003-2013. See also Sect. 4.3.

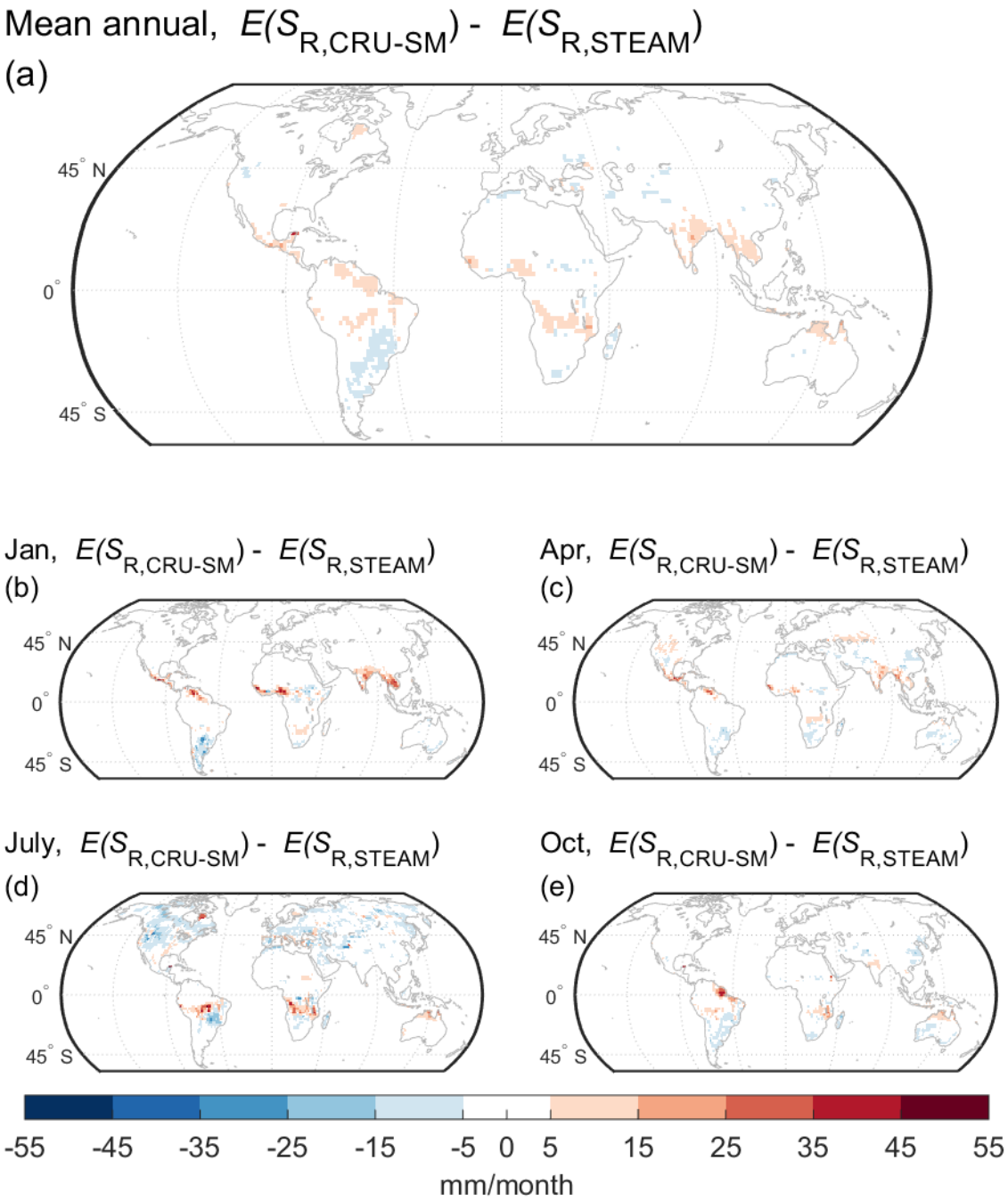

Figure S11. Difference in STEAM-simulated evaporation between using $S_{R,CRU\text{-}SM}$ and $S_{R,STEAM}$ as root zone storage capacity parametrisation at (a) mean annual scale and averages for the months of (b) January, (c) April, (d) July, and (e) October over the time period 2003-2013. (This figure is the same as Fig. 6 in the main paper, but a different colour scale for ease of comparison with Fig. S10.)

References

de Boer-Euser, T., McMillan, H. K., Hrachowitz, M., Winsemius, H. C. and Savenije, H. H. G.: Influence of soil and climate on root zone storage capacity, Water Resour. Res., doi:10.1002/2015WR018115, 2016.

Canadell, J., Jackson, R. B., Ehleringer, J. B., Mooney, H. a., Sala, O. E. and Schulze, E.-D.: Maximum rooting depth of vegetation types at the global scale, Oecologia, 108(4), 583–595, doi:10.1007/BF00329030, 1996.

Collins, D. B. G. and Bras, R. L.: Plant rooting strategies in water-limited ecosystems, Water Resour. Res., 43(6), W06407, doi:10.1029/2006WR005541, 2007.

van Dijk, A., Warren, G., Van Niel, T., Byrne, G., Pollock, D. and Doody, T.: Derivation of data layers from medium resolution remote sensing to support mapping of groundwater dependent ecosystems., 2014.

Fenicia, F., Savenije, H. H. G. and Avdeeva, Y.: Anomaly in the rainfall-runoff behaviour of the Meuse catchment. Climate, land-use, or land-use management?, Hydrol. Earth Syst. Sci., 13(9), 1727–1737, doi:10.5194/hess-13-1727-2009, 2009.

Gao, H., Hrachowitz, M., Schymanski, S. J., Fenicia, F., Sriwongsitanon, N. and Savenije, H. H. G.: Climate controls how ecosystems size the root zone storage capacity at catchment scale, Geophys. Res. Lett., 41(22), 7916–7923, doi:10.1002/2014GL061668, 2014.

van Genuchten, M. T.: A Closed-form Equation for Predicting the Hydraulic Conductivity of Unsaturated Soils, Soil Sci. Soc. Am. J., 44, 892–898, doi:10.2136/sssaj1980.03615995004400050002x, 1980.

Ichii, K., Hashimoto, H., White, M. a., Potter, C., Hutyra, L. R., Huete, A. R., Myneni, R. B. and Nemani, R. R.: Constraining rooting depths in tropical rainforests using satellite data and ecosystem modeling for accurate simulation of gross primary production seasonality, Glob. Chang. Biol., 13(1), 67–77, doi:10.1111/j.1365-2486.2006.01277.x, 2007.

Jackson, R. B., Canadell, J., Ehleringer, J. R., Mooney, H. A., Sala, O. E. and Schulze, E. D.: A global analysis of root distributions for terrestrial biomes, Oecologia, 108(3), 389–411, doi:10.1007/BF00333714, 1996.

Kleidon, A.: Global datasets of rooting zone depth inferred from inverse methods, J. Clim., 17(13), 2714–2722, doi:10.1175/1520-0442(2004)017<2714:GDORZD>2.0.CO;2, 2004.

Laio, F., D'Odorico, P. and Ridolfi, L.: An analytical model to relate the vertical root distribution to climate and soil properties, Geophys. Res. Lett., 33(18), L18401, doi:10.1029/2006GL027331, 2006.

Matsumoto, K., Ohta, T., Nakai, T., Kuwada, T., Daikoku, K., Iida, S., Yabuki, H., Kononov, A. V., van der Molen, M. K., Kodama, Y., Maximov, T. C., Dolman, A. J. J. and Hattori, S.: Responses of surface conductance to forest environments in the Far East, Agric. For. Meteorol., 148(12), 1926–1940, doi:10.1016/j.agrformet.2008.09.009, 2008.

Müller Schmied, H., Eisner, S., Franz, D., Wattenbach, M., Portmann, F. T., Flörke, M. and Döll, P.: Sensitivity of simulated global-scale freshwater fluxes and storages to input data, hydrological model structure, human water use and calibration, Hydrol. Earth Syst. Sci., 18(9), 3511–3538, doi:10.5194/hess-18-3511-2014, 2014.

Schenk, H. J.: The shallowest possible water extraction profile: a null model for global root distributions, Vadose Zo. J., 7(3), 1119, doi:10.2136/vzj2007.0119, 2008.

Schenk, H. J. and Jackson, R. B.: ISLSCP II Ecosystem rooting depths, in ISLSCP Initiative II Collection, edited by F. G., G. Collatz, B. Meeson, S. Los, E. B. de Colstoun, and D. Landis, Oak Ridge National

Laboratory Distributed Active Archive Center, Oak Ridge, Tennessee, U.S.A., 2009.

Wang-Erlandsson, L., van der Ent, R. J., Gordon, L. J. and Savenije, H. H. G.: Contrasting roles of interception and transpiration in the hydrological cycle – Part 1: Temporal characteristics over land, Earth Syst. Dyn., 5(2), 441–469, doi:10.5194/esd-5-441-2014, 2014.

van Wijk, M. T. and Bouten, W.: Towards understanding tree root profiles: simulating hydrologically optimal strategies for root distribution, Hydrol. Earth Syst. Sci., 5(4), 629–644, doi:10.5194/hess-5-629-2001, 2001.

Winsemius, H. C., Schaefli, B., Montanari, A. and Savenije, H. H. G.: On the calibration of hydrological models in ungauged basins: A framework for integrating hard and soft hydrological information, Water Resour. Res., 45(12), W12422, doi:10.1029/2009WR007706, 2009.